

Q. Xu

*Research Reactor Institute, Kyoto University*

**OBJECTIVES:** Neutron irradiation is usually used to investigate radiation effects in solid materials and develop new materials. Unfortunately, because the operation time of KUR was limited, and the laboratory for neutron-irradiated samples could not be used in 2014, the research activities were severely restricted. In the present report, instead of neutron irradiation, ion, electron and  $\gamma$  ray irradiations were used to estimate degradation mechanical properties of materials, such as material for optoelectronic and high-power devices.

**RESULTS:** The allotted research subject (ARS) and the name of co-researchers in each ARS are listed below.

## ARS-1

Compensation mechanism of DX-like center in neutron transmutation doped GaN

(K. Kuriyama, T. Nakamura, A. Shikawa, K. Kushida, and Q. Xu)

## ARS-2

Neutron irradiation effects of superconducting magnet materials at low temperature

(T. Nakamoto, M. Yoshida, T. Ogitsu, Y. Makida, K. Sasaki, S. Mihara, K. Yoshimura, H. Nishiguchi, M. Sugano, M. Iio, Y. Yang, Y. Kuno, M. Aoki, A. Sato, Q. Xu, K. Sato, Y. Kuriyama and Y. Mori)

Candidate materials, such as Al and Cu alloys, for superconducting magnets of upgraded LHC at CERN and the muon source for the COMET experiment at J-PARC were irradiated by LTL at  $\sim 10$  K. In Al alloys, almost 100% of the defects produced by the irradiation was recovered after warming up to room temperature, however, several percent of the defects was remained in Cu alloy even at room temperature.

## ARS-3

Study on fine structures formed by high energy particle irradiation

(A. Kinomura, K. Sato, Q. Xu and T. Yoshiie)

## ARS-4

Thermoluminescence of Synthesized Calcite

(T. Awata, K. Nakashima and Q. Xu)

## ARS-5

Electron irradiation on W at around 500 °C using KURRI-LINAC

(M. Akiyoshi, T. Yoshiie, Q. Xu and K. Sato)

## ARS-6

The development of new positron beam system using KUR

(Y. Nagai, K. Inoue, T. Toyama, Y. Shimizu, K. Nagumo, M. Shimodaira, T. Hirota, K. Sato, T. Yoshiie and Q. Xu)

## ARS-7

Radiation damage in bulk amorphous alloys by electron irradiation

(F. Hori, K. Ishii, T. Ishiyama, K. Kobayashi, A. Iwase, Y. Yokoyama, Q. Xu and K. Sato)

## ARS-10

Positron annihilation study of Fe-Cr alloys after neutron irradiation in KUR

(R. Kasada, K. Sato and Q. Xu)

## ARS-12

Positron annihilation lifetime measurements austenitic stainless steels irradiated in the SINQ target irradiation program

(K. Sato, Q. Xu, T. Yoshiie, Y. Dai and K. Kikuchi)

## ARS-13

Effects of high energy particle irradiation on hydrogen retention in refractory metals

(K. Tokunaga, M. Matsuyama, S. Abe, H. Osaki, K. Araki, T. Fujiwara, M. Hasegawa, K. Nakamura, Q. Xu and K. Sato)

## ARS-14

Dependence of cellular structure formation on ion species

(N. Nitta, C. Watanabe, M. Taniwaki, Q. Xu and T. Yoshiie)

**CONCLUSIONS:** The defects induced by irradiation degrade the physical mechanical properties of solid materials. Part of the physical and mechanical properties can be recovered at high temperatures where defects are mobile. Some experimental results are important for development of large equipment. For example, the results of ARS-2 indicate that Al alloys can be used in high energy, high-power accelerator as the material of superconducting magnets since the defects produced by the irradiation recover when the magnets are warmed up to room temperature.

## PR6-1 Compensation Mechanism of DX-like Center in Neutron Transmutation Doped GaN

K. Kuriyama, T. Nakamura, A. Shinkawa, K. Kushida<sup>1</sup>, and Q. Xu<sup>2</sup>

College of Engineering and Research Center of Ion Beam Technology, Hosei University

<sup>1</sup>Osaka Kyoiku University

<sup>2</sup>Research Reactor Institute, Kyoto University

**INTRODUCTION:** The 1000 °C annealed neutron transmutation doped (NTD)-GaN keeps having high resistivity of  $10^8 \Omega\text{cm}$  at room temperature. In the present study, we report the compensation mechanism of DX-like center of the neutron transmuted Ge in NTD-GaN.

**EXPERIMENTS:** GaN epitaxial films on sapphire substrates were irradiated with fast and thermal neutrons at fluences of  $6.7 \times 10^{18} \text{ cm}^{-2}$  and  $1.4 \times 10^{19} \text{ cm}^{-2}$ , respectively. We carried out an alternating current (ac)-Hall effect measurement and clarified the existence of deep energy level from the temperature dependence of carrier concentration in high temperature region.

**RESULTS:** The resistivity and carrier concentration of the 1000 °C annealed samples were  $2.47 \times 10^6 \Omega\text{cm}$ ,  $4.13 \times 10^{10} \text{ cm}^{-3}$  at 150 °C and  $2.37 \times 10^3 \Omega\text{cm}$ ,  $1.60 \times 10^{14} \text{ cm}^{-3}$  at 400 °C, respectively. All annealed samples showed the n-type conduction. The carrier concentration at both 150 °C and 400 °C were much lower than the calculated transmuted-Ge concentration ( $1.24 \times 10^{18} \text{ cm}^{-3}$ ). Fig. 1 (a) and (b) show the schematic diagram of impurity levels of NTD-GaN. Ge atoms transmuted in GaN by the two (n, $\gamma$ ) reactions of  $^{69}\text{Ga}$  and  $^{71}\text{Ga}$  form the DX-like center as donor [1]. Ge is localized at 500 meV below the bottom of the conduction band from results of photoluminescence (PL) measurements [1], supporting the results of the theoretical calculation [2]. N interstitial ( $\text{N}_i$ ) atoms generated by NTD-process form the deep acceptor level at 960 meV below the bottom of the conduction band from present study.  $^{14}\text{C}$  atoms generated by the (n,p) reaction are substituted to N sites and forms the acceptor level at 230 meV above the top of the valence band [3], consistent with the result from the PL measurements[4]. Since the carrier concentration of NTD-GaN cannot be measured at room temperature, DX-like center of Ge is compensated by both  $^{14}\text{C}$  and  $\text{N}_i$  acceptors. The Fermi level estimated from the following equation [5] for a temperature range of 150 - 400 °C was  $650 \pm 25 \text{ meV}$ .

$$n = 2(m_e k_B T / 2\pi\hbar^2)^{3/2} \exp[(E_F - E_g) / k_B T],$$

where  $m_e$  is the effective mass of GaN,  $k_B$  the Boltzmann's constant. Therefore, the increase of the carrier concentration with increasing the temperature would be attributed to the thermal excitation to the conduction band of electrons trapped in  $\text{N}_i$  acceptors, as shown in Fig. 1 (b).

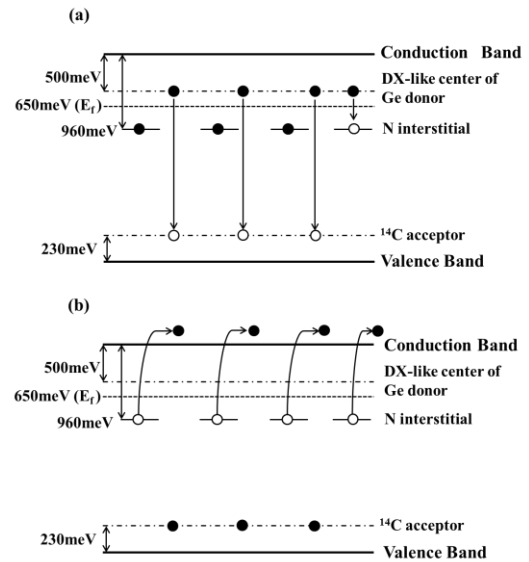


Fig 1. The schematic diagram of impurity levels in NTD-GaN. (a) the compensation of DX-like center of Ge donors by  $^{14}\text{C}$  and  $\text{N}_i$  acceptors. (b) the thermal excitation from the energy level of N interstitial.

A part of KURRI Progress Report has been published in Solid State Communications, 205, 1 (2015).

### REFERENCES:

- [1] K. Kuriyama, T. Tokumasu, Jun Takahashi, H. Kondo, and M. Okada, Appl. Phys. Lett. 80, 3328 (2002); Proceedings of 26th Int. Conf. Physics of Semiconductors (Edinburgh, UK) D46 (2002).
- [2] P. Boguslawski, J. Bernholc, Phys. Rev. B 56, 9496 (1997).
- [3] J. Neugebauer, C. G. Van de Walle, Phys. Rev. B 50, 8067 (1994).
- [4] T. Ida, T. Oga, K. Kuriyama, K. Kushida, Q. Xu, and S. Fukutani, AIP Conference Proceedings, 1566, 67 (2013) (31st Int. Conf. Physics of Semiconductors, Zurich, Switzerland, 2012).
- [5] G. Burns, in Solid State Physics, (Academic Press, Inc, 1985) Chap.2.

採択課題番号 26P6-1 化合物半導体の照射効果と電氣的・光学的物性に関する研究 プロジェクト  
(法政大院) 栗山一男、中村 司、新川 輝、(大阪教育大) 串田一雅  
(京大・原子炉) 徐 虬

T. Nakamoto, M. Yoshida, T. Ogitsu, Y. Makida, K. Sasaki, S. Mihara, K. Yoshimura, H. Nishiguchi, M. Sugano, M. Iio, Y. Yang<sup>1</sup>, Y. Kuno<sup>2</sup>, M. Aoki<sup>2</sup>, A. Sato<sup>2</sup>, Q. Xu<sup>3</sup>, K. Sato<sup>3</sup>, Y. Kuriyama<sup>3</sup>, and Y. Mori<sup>3</sup>

J-PARC Center, KEK

<sup>1</sup>Department of Applied Quantum Physics & Nuclear Engineering, Kyushu University

<sup>2</sup>Department of Physics, Osaka University

<sup>3</sup>Research Reactor Institute, Kyoto University

**INTRODUCTION:** Superconducting magnets will be subjected to a high neutron fluence of  $10^{21}$  n/m<sup>2</sup> or higher in the operation lifetime in the high energy particle physics experiments, such as a high luminosity upgrade of the LHC at CERN and the muon source for the COMET experiment at J-PARC. Since electrical resistivity of a stabilizer at low temperature, which is very sensitive to neutron irradiation, is one of the important parameters for the quench protection of the magnet system. A series of electrical resistivity measurement at neutron irradiation for the aluminum stabilizer with additives of yttrium taken from the prototype superconducting cable as well as copper stabilizer was started in 2011. In 2014, the fourth irradiation test with the same samples which were irradiated so far was performed to observe the effect of the multiple irradiations and the thermal cycles to room temperature on the electrical resistivity.

**EXPERIMENTS:** The irradiation tests have been carried out at a low temperature irradiation facility (LTL) at E-4 line of KUR. Detailed experimental procedure was reported in [1]. The aluminum stabilizer samples with dimensions of 1 mm x 1 mm x 70 mm were cut from the superconducting cable manufactured by Hitachi Cable. The copper stabilizer sample has the dimensions of  $\phi$ 1mm x 50mm. The electric resistance was measured by a 4-wire method employing a Keithley 6221 current source and a Keithley 2182A voltmeter. The temperature was determined by using a thermocouple of Au(Fe) and Chromel, since the Cernox sensor (CX-1050-SD for

2011 - 2013, CX-1070-SD for 2013 - 2014) showed a temperature drift during neutron exposure due to the irradiation damage. The thermocouple and the Cernox sensor were placed just behind the samples to measure the temperature of the helium gas coolant.

**RESULTS:** The fourth irradiation test for the aluminum sample (Al-Y2) and the copper sample was carried out in April 2014. Another type of aluminum sample with Ni additive (Al-Ni) was also irradiated at second time. The irradiation condition is basically same as the previous irradiations. After cooling down to 12 K, the reactor was turned on to a power of 1 MW. The estimated fast neutron fluence in 53.5 hours operation is  $2.7 \times 10^{20}$  n/m<sup>2</sup>. Behavior of the induced resistance by the neutron irradiation is very similar to the previous results. Degradation rates of the electrical resistivity for both aluminum samples are quite similar:  $2.2 \times 10^{-31} \Omega\text{m}^3$  and  $2.3 \times 10^{-31} \Omega\text{m}^3$  for Al-Y2 and Al-Ni, respectively. For copper sample, the degradation rate is  $7.3 \times 10^{-31} \Omega\text{m}$ . After the irradiation, all samples were warmed up to room temperature. Anneal effects of the samples were measured at the subsequent cooling test to 12 K in December 2014 without irradiation. Table 1 lists the summary of irradiation tests so far. For the aluminum samples, the induced resistance was fully recovered to be the original resistance for all cases while the degradation rate is much higher than copper. This means that the degraded electrical resistivity of aluminum stabilizer in the superconducting magnet due to the irradiation can be completely recovered by the adequate intervention of warming up to room temperature. For the copper sample, however, the recovery of the resistance by the thermal cycle was imperfect for all cases: the recovery rates were 82 % to 96 %. This will concern the safe operation of the superconducting magnet at severe radiation environment.

#### REFERENCES:

[1] M. Yoshida *et al.*, Proc. of ICEC 24-ICMC 2012, 685-688, 2013.

Table 1. Summary of irradiation effects on electrical resistivity of stabilizers with multiple neutron irradiations.

Sample, irradiation year	Initial RRR	T <sub>irr</sub> (K)	$\Phi_{\text{tot}} (>0.1 \text{ MeV})$ (n/m <sup>2</sup> )	$\Delta\rho_{\text{irr}}/\Phi_{\text{tot}} \times 10^{-31}$ ( $\Omega\text{m}^3$ )	Recovery Rate (%)	
Al-Y2	2011	360	12	$2.6 \times 10^{20}$	2.8	100
	2012	360	15	$2.6 \times 10^{20}$	2.9	100
	2013	368	15	$2.6 \times 10^{20}$	2.5	100
	2014	367	14	$2.7 \times 10^{20}$	2.2	100
Al-Ni	2013	561	15	$2.6 \times 10^{20}$	2.6	100
	2014	566	14	$2.7 \times 10^{20}$	2.7	100
Copper	2011	308	12	$2.6 \times 10^{20}$	0.93	82
	2012	291	15	$2.6 \times 10^{20}$	1.02	92
	2013	285	15	$2.6 \times 10^{20}$	0.77	95
	2014	277	14	$2.7 \times 10^{20}$	0.73	96

## PR6-3 Study on Fine Structures Formed by High Energy Particle Irradiation

A. Kinomura\*, K. Sato<sup>1</sup>, Q. Xu<sup>1</sup> and T. Yoshiie<sup>1</sup>

National Institute of Advanced Industrial Science and Technology (AIST)

<sup>1</sup>Research Reactor Institute, Kyoto University

\*Present address: Research Reactor Institute, Kyoto University

**INTRODUCTION:** The effects of ion irradiation have been extensively studied for various crystalline materials. It is known that irradiation causes the damage of crystallinity, leading to the degradation of original material properties. However, under particular irradiation conditions, the irradiation effects can induce interesting phenomena such as ion beam annealing in Si, where crystallinity of implantation-induced damage layers are recovered by other ion irradiation. Thus, it is important to investigate the irradiation effects of energetic particles (ions and neutrons) and the influence on crystallinity of materials.

**EXPERIMENTS:** Neutron enhanced annealing (crystalline recovery) of ion-implantation induced damage in single-crystalline Si has been investigated to compare the difference in annealing effects between ion and neutron irradiations. Si ion implantation to (100)-oriented Si was performed at 200 keV to a dose of  $5 \times 10^{14} \text{ cm}^{-2}$  to introduce irradiation damage in the sample. The Si-implanted sample was encapsulated in an Al capsule with He ambient gas and neutron irradiated for 12 weeks in the core irradiation facility of the Kyoto University Reactor (KUR) operating at 5 MW. Control samples were thermally annealed at 90 °C in a quartz tube furnace with flowing Ar gas for the same annealing time as the neutron irradiation. The damage levels of samples were measured by Rutherford backscattering with channeling (RBS/C) using a 2 MeV He ion beam.

**RESULTS:** Sample temperatures cannot be directly measured during reactor operation in the case of the KUR core irradiation facility. In this study, the sample temperature during the neutron irradiation was estimated to be below 90 °C by solving a partial differential equation describing the heat flow inside the sample capsule made of Al. Since the thermal annealing rate for heavily damaged Si was nearly constant around 90 °C, the error of estimated temperature rise does not affect the result of this irradiation experiment.

The samples before and after irradiation were measured and damage levels were calculated by taking account of dechanneling fractions in RBS/C spectra. Annealing efficiencies obtained in this and previous studies [1, 2] were plotted (closed circles), under the assumption that the irradiation temperature in this study was 90 °C. For comparison, efficiencies of ion beam annealing of disorder were also calculated from the data by other groups and plotted in Fig. 4 (closed square and

triangle), where the room temperature was assumed to be 27 °C.

Types of major annealed defects are different depending on the irradiation temperature in the current temperature range (from room temperature to 400 °C). Damage peak after thermal annealing at 400 °C was close to the undamaged level in the RBS/C spectrum, whereas the damage peak after thermal annealing at 90 °C (in this study) was close to the random level. In spite of the difference in annealed defects, the Arrhenius plot provides some insights in terms of the comparison between neutron-enhanced and ion-beam annealing. The difference in efficiency between neutron-enhanced and ion-beam annealing was within one order of magnitude, implying that a similar mechanism may be at work for both of annealing methods.

In summary, the effect of neutron irradiation on ion-implantation induced damage in Si was investigated using the neutron irradiation in KUR. Similar annealing efficiencies were obtained for neutron-enhanced and ion-beam annealing experiments.

**ACKNOWLEDGMENT:** We would like to thank K. Yasuda and R. Ishigami of the Wakasa Wan Energy Research Center and colleagues of AIST for their assistance on this study.

### REFERENCES:

- [1] A. Kinomura, T. Yoshiie, A. Chayahara, Y. Mokuno, N. Tsubouchi, Y. Horino, Q. Xu, K. Sato, K. Yasuda, and R. Ishigami, Nucl. Instrum. Methods Phys. Res. B 334 (2014) 48.
- [2] A. Kinomura, A. Chayahara, Y. Mokuno, N. Tsubouchi, Y. Horino, T. Yoshiie, Y. Hayashi, Q. Xu, Y. Ito, R. Ishigami and K. Yasuda, Appl. Phys. Lett. 88 (2006) 241921.

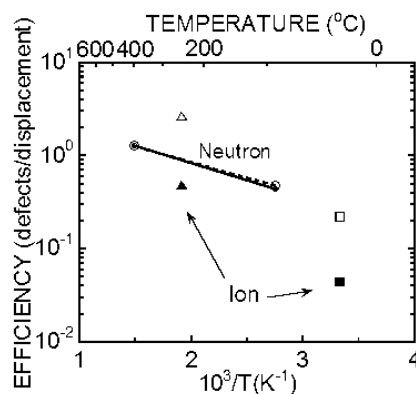


Fig. 1 Annealing efficiencies of neutron and ion-beam irradiations. Closed circles (neutron), triangle and square (ion) correspond to the original efficiencies. Open circles (neutron), triangle and squares (ion) correspond to the efficiencies corrected based on displacement-rate dependence.

T. Awata, K. Iwasaki, S. Tanaka, Q. Xu<sup>1</sup>

Department of Physics, Naruto University of Education  
<sup>1</sup>Research Reactor Institute, Kyoto University

**INTRODUCTION:** We reported that thermoluminescence (TL) of natural calcite ( $\text{CaCO}_3$ ) irradiated by gamma rays [1-2]. In that result, it was shown that the almost spectra of TL had only one orange emission peak at 620nm, and that may be originated from a small amount of impurity of  $\text{Mn}^{2+}$  in Calcite [3]. In this study, we have artificially synthesized calcite with different kinds of impurity using chemical reaction in water solution, and compared TL spectra of these with natural calcite, and to clear the relationship with emission and kinds of impurity.

**EXPERIMENTS:** Calcites were synthesized by a chemical reaction method in water solution [4]. 1.5% of  $(\text{NH}_4)_2\text{CO}_3 \cdot \text{H}_2\text{O}$  (1.5g in 100mL pure water) and 1.8% of  $\text{CaCl}_2 \cdot 6\text{H}_2\text{O}$  (2g in 100mL pure water) with 0.01g element impurity were mixed at room temperature. After mixed, these solutions were precipitated by holding for two weeks, and filtering. After filtering, samples were shaped by a tablet machine. We have made three samples with different element impurities (Mn, Mn+Ce, Mn+Pb). These samples were irradiated  $^{60}\text{Co}$  gamma rays for 1h (about 20kGy) at 77K using KUR gamma-ray facility. The thermoluminescence spectra were measured by a photo-spectrometer (Princeton Instrument Spectra Pro 300i) with a temperature controlled system (77K to 413K).

**RESULTS and DISCUSSION:** Figure 1 shows the thermoluminescence picture of synthesized calcite with an impurity Mn and Mn+Ce by gamma rays irradiation. This picture was taken by stereo microscope after pick-

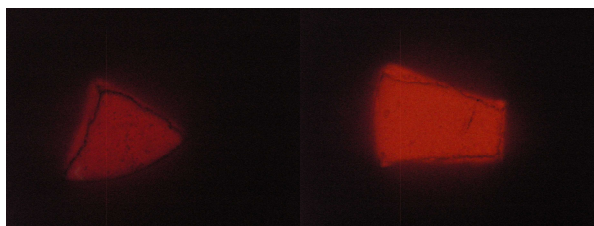


Fig. 1 Thermoluminescence of synthesized calcite with an impurity of Mn (left) and Mn+Ce (right).

ing out from liquid nitrogen. Both pictures show orange emission almost same as natural calcite with Mn element [2]. Figure 2 shows a 3D thermoluminescence spectrum of calcite with Mn impurity irradiated by  $\gamma$  rays at 77K from 93K to 413K with heating speed at 0.32K/second.

X-, Y- and Z- axes indicate emission wavelength (nm) of emission, temperature and intensity, respectively. There is one peak at 620nm starting from 285K same result as

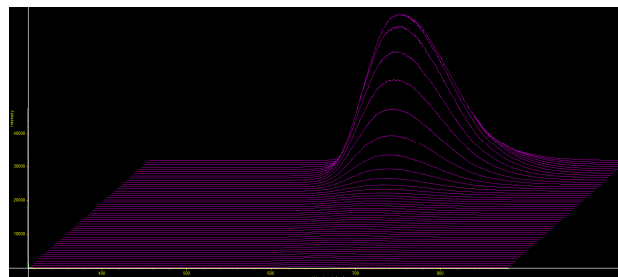


Fig. 2 TL 3D spectrum of synthesized calcite with Mn irradiated by gamma rays.

former our experiment of natural calcite [2]. It is clear that 620nm emission peak at calcite is originating from existence of small amount of Mn. This result is supported by study of Medlin [3]. Figure 3 shows those TL spectra of synthesized calcite with Mn, Mn+Ce and Mn+Pb at maximum intensity temperature. Mn and Mn+Pb spectra looks alike, and have one peak at 620nm same as former our experiment. As Mn+Ce spectra, it has one peak at 640nm which is different from other two samples. Comparing this result with photoluminescence one makes it possible to be clear that reason.

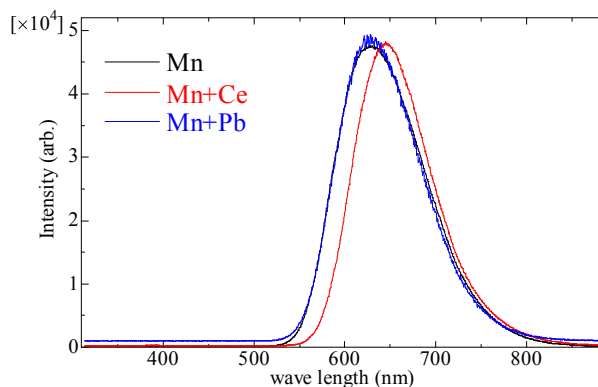


Fig.3 TL spectra of synthesized calcite with Mn, Mn+Ce and Mn+Pb.

#### REFERENCES:

- [1] T. Awata, T. Kishino, F. Maki and Q. Xu, KURRI Progress Report **2011**, p.143.
- [2] T. Awata, K. Nakashima and Q. Xu, KURRI Progress Report **2013** p.169.
- [3] W. L. Medlin, *J. Opt. Soc. Am.* **53**(1963)1276.
- [4] G. R. Fonda, *J. Phys. Chem.* **44**(1940)435.

M. Akiyoshi<sup>1</sup>, T. Yoshiie<sup>2</sup>, Q. Xu<sup>2</sup>, K. Sato<sup>2</sup>

<sup>1</sup>Faculty of Engineering, Kyoto University  
(from 2015.04: Radiation Research Center, Osaka Prefecture University)

<sup>2</sup>Research Reactor Institute, Kyoto University

### INTRODUCTION:

It is well known that irradiation induced damages in ceramics showed significant degradation in thermal diffusivity unlike metals. In addition, the dependence of thermal diffusivity on measurement temperature is affected with irradiation induced damages. Therefore, thermal diffusivity during the irradiation is still not estimated. To resolve this problem, kinetic analysis is required where most important information is the behavior of point defects. Electron irradiation is the best choice to induce simple Frenkel pairs.

In these days, W (tungsten) material is considered as a candidate for divertor material in future fusion reactor. W is metal, of course, but showed a similar behavior of thermal diffusivity. It shows relatively small thermal diffusivity arisen from low electron conductivity, but shows dependence on measurement temperature like ceramics caused by phonon-phonon scattering.

In this study, we irradiated W specimen using KURRI-LINAC and check the specimen temperature during the irradiation, and also radio-activity of specimens.

### EXPERIMENTS:

In the previous work, 30MeV electron accelerator KURRI-Linac is used to induce point-defects in bulk specimens of typical structural ceramics to  $1.5 \times 10^{24} \text{e/m}^2$  which correspond to 0.01dpa in typical ceramics. The irradiation was performed in a new irradiation system constructed to achieve an irradiation at around 400°C where interstitial atoms have enough mobility to migrate.

In the previous work, ceramic specimens were irradiated using this irradiation system. In the system, a specimen is settled in a Cu specimen-holder, and holders are piled between Cu heat spread plates and graphite heat spread seats. Usually, a graphite seat spreads heat well horizontally, but the graphite seat in this system is 'Vertical-Graphite' (produced by Hitachi Chemical) of which thermal conductivity vertical to the seat is  $90 \text{W/m} \cdot \text{K}$ . This vertical-graphite sheet was 0.15mm in thickness and was cut into  $\phi 10$  that cover the specimen to have good thermal contact on the surface. In conventional system, heat contact is achieved by thermal grease that contains Ag powders. But in this system, neutrons from photo-

nuclear reaction will activate Ag atoms very strongly, so it cannot be used. In addition, conventional (horizontal) graphite sheet (Panasonic PGS graphite sheet, EYGS-182310  $t=0.10\text{mm}$ ,  $TC=700\text{W/m} \cdot \text{K}$ ) is used to spread heat horizontally.

The piled graphite sheets and specimen holders are tighten with screws and nuts made by Ti to avoid radio activation. This pile is put between Al square tubes with the vertical-graphite seats. All specimens and Cu plates are coated by BN spray to avoid surficial oxidation. In addition, a Cu aperture was put in front of the specimen pile to trim down the beam irradiated on out side of the specimen that heats the pile wastefully.

Pure W specimens (Nilaco) was cut into  $\phi 10$  and the thickness was 0.5mm (2 pieces) and 1.0mm (1 piece).  $\alpha$ - $\text{Al}_2\text{O}_3$ ,  $\beta$ -SiC specimens ( $\phi 10 \times 0.5\text{mm}$ ) are also irradiated.

### RESULTS:

The beam condition was Acc. Energy: 32MeV, Pulse length  $4\mu\text{s}$ , Peak current: 550mA. The frequency was once increased to 110Hz, but specimens showed a trend of over heating, so the frequency was settled down to 100Hz. Even at that frequency, the total beam energy was 7.0kW in several  $\text{cm}^2$  that can compare with the heat flux on divertor in the fusion reactor ITER which is planed as  $10\text{MW/m}^2$ . This irradiation system got over this high heat flux and achieved reliable irradiation at around 550°C.

The irradiation damage induced by the electron irradiation is calculated. For the most ceramics,  $2.82 \times 10^{20}$  electrons in  $2\text{cm}^2$  accelerated to 32MeV induces defects up to  $1.00 \times 10^{-2} \text{dpa}$  (target mass  $M=16\text{amu}$ , atomic number  $Z=8$ , knock on energy  $E_d=30\text{eV}$ ). W is far heavier ( $M=183.8\text{amu}$ ) and knock on energy is larger ( $E_d=100\text{eV}$ ), but the collision cross section is 48.4barn while ceramics shows only 18.7barn. It is said that the  $E_d$  of W is a little smaller, and if it is 80eV, the cross section is 60.1barn. Therefore, induced damage in W is larger than typical ceramics,  $1.48 \times 10^{-2} \text{dpa}$  ( $E_d: 100\text{eV}$ )  $\sim 1.95 \times 10^{-2} \text{dpa}$  ( $E_d: 80\text{eV}$ ).

After the irradiation, radio-activity of the specimen holder and specimens was investigated. The whole irradiation holder showed over 100mSv/h in the surface at 17h after the beam stop, 55mSv/h at 33h and 38mSv/h at 40h that corresponds  $t_{1/2} = 13.7\text{h}$ . The half-time of W-185 is 75.1day and W-187 is 23.7h while Cu-64 is 12.7h, so the most of the activity was assumed to be arisen from Cu-64.

Y. Nagai, K. Inoue, T. Toyama, Y. Shimizu, K. Nagumo, M. Shimodaira, T. Hirota, K. Sato<sup>1</sup>, T. Yoshiie<sup>1</sup>, Q. Xu<sup>1</sup>  
*Institute for Materials Research, Tohoku University,*  
<sup>1</sup>*Research Reactor Institute, Kyoto University*

**INTRODUCTION:** Positron annihilation spectroscopy is well-known to be a powerful tool to detect vacancy-type defects. In 2000 years, it is found that the positron is also sensitive to (sub)nano embedded particles (SNEPs) with higher positron affinities than that of the host, even if the SNEPs are free from open-volume defects. The representative case is ultrafine Cu precipitates in Fe.

We are developing a new positron annihilation apparatus, positron age-momentum correlation (AMOC), to study the correlation between the Cu precipitates and the vacancy-type defect induced by neutron irradiation in the light water reactor pressure vessel (RPV) steels, which is important to understand the irradiation induced embrittlement of the RPV steels due to long-term in-service exposure to neutron irradiation. For this study, an intense positron source is required to achieve higher count rates because typically it takes more than one week for one spectrum by the conventional AMOC system using <sup>22</sup>Na positron source.

In this work, a new positron beam facility with high positron intensity is constructed at the Kyoto University Research Reactor (KUR), which is the first reactor based positron beam in Japan[1].

**EXPERIMENTS and RESULTS:** An in-pile positron source was installed at the B-1 hole (20 cm in diameter) in KUR. The positron beam line consists of two parts: one is located inside the reactor, and the other is located outside the reactor as shown in Fig. 1 [1,2]. Positrons are generated by pair production from high-energy  $\gamma$ -rays. The  $\gamma$ -ray flux and the thermal neutron flux at the positron source position are about  $1.5 \times 10^{12}$  n/cm<sup>2</sup> and  $10^5$  Gy/h, respectively, at 5 MW. A W converter of 1 mm thick and 3 cm diameter and W moderators with a Cd shroud are used to obtain slow positrons as shown in Fig. 2. In order to enhance the positron generation, a 1 mm thick Cd shroud covered with an Al plate was mounted on the top of the magnetic field to cap the converter and moderator, because high energy  $\gamma$ -ray are generated by the <sup>113</sup>Cd(n,  $\gamma$ )<sup>114</sup>Cd reaction. The moderators were annealed after the W strips were set in lattices. When annealing, they were encased in covered boxes of 50  $\mu$ m-thick W foil and the boxes were irradiated on the covering lids with electron beam welder at KEK in Tsukuba [3]. The annealing temperature was elevated to approximately 2400°C. The vacuum of the welder chamber was about  $10^{-5}$  torr. The slow positrons emitted from the moderator were subsequently accelerated up to 30 eV and confined magnetic fields of several mT. In order to eliminate the background of fast neutrons and  $\gamma$ -rays from the reactor core, the slow positron beam passes two bends in shields consisting of polyethylene, concrete and lead

blocks. After passing the bends, the slow positrons are transported to sample chamber at an energy up to 20 keV.

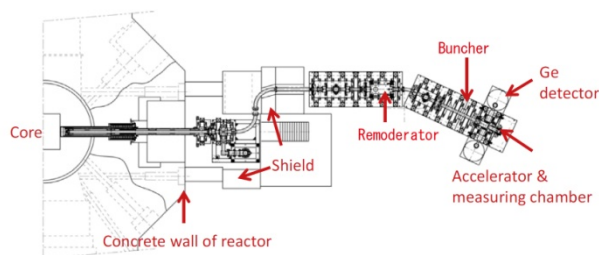


Figure 1: A schematic diagram of KUR positron beam system [1,2].

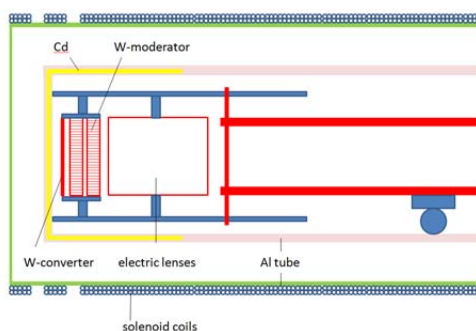


Figure 2: A schematic diagram of the in-pile positron source at KUR [1,2].

Figure 3 shows the positron beam spot recorded using a microchannel plate (MCP). The beam has a slightly elliptical shape and the major and minor axes have length about 2.0 and 1.5cm, respectively. The lattice structure of W moderator is clearly visible. The positron beam intensity is determined about  $10^6$  e<sup>+</sup>/s at 1 MW by Ge detector.

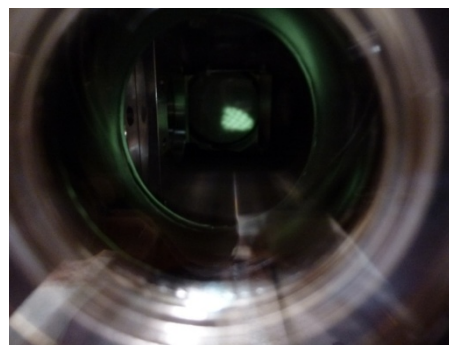


Figure 3: The observation of positron beam from KUR using microchannel plate.

#### REFERENCES:

- [1] Q Xu *et al*, J. Phys. Conf. Ser. **505** (2014) 012030.
- [2] K Sato *et al*, Nucl. Inst. Meth. Phys. Resear. B **342** (2015) 104.
- [3] K Wada *et al*, Eur. Phys. J. D **66** (2012) 37.

採択課題番号 26P6-6 KUR を用いた新しい陽電子源の開発と材料研究への応用 プロジェクト  
 (東北大・金研) 永井康介、井上耕治、外山健、清水康雄、南雲一章、下平昌樹、廣田太一  
 (京大・原子炉) 義家敏正、徐虬、佐藤紘一

## PR6-7 Radiation Damage in Bulk Amorphous Alloys by Electron Irradiation

F.Hori, K.Ishii, T.Ishiyama, K.Kobayashi, A.Iwase,  
Y.Yokoyama<sup>1</sup>, Q.Xu<sup>2</sup> and K.Sato<sup>2</sup>

*Dept. of Mater. Sci., Osaka Prefecture University*

<sup>2</sup>*Institute of Materials Research, Tohoku University*

<sup>1</sup>*Research Reactor Institute, Kyoto University*

**INTRODUCTION:** Bulk amorphous alloys are expected to be useful for various applications because they have superior mechanical properties such as strength, hardness and corrosion resistance. We have been suggested that the properties of bulk glassy alloys can be improved by high energetic particles irradiation. So far, we have reported that effects of free volume and mechanical properties on the bulk amorphous alloys depend upon the irradiation species [1,2]. Also change in free volume by the irradiation strongly reflects various properties such as hardness and ductility of bulk amorphous alloys. Recent years, eutectic ZrCuAl bulk glassy alloy shows the degradation of ductility and toughness by annealing but that for hypoeutectic remains unchanged after annealing. In order to estimate irradiation effects for various compositional bulk amorphous alloys, we performed electron irradiation for various kinds of ZrCuAl bulk amorphous alloys. Before and after irradiation, we have examined X-ray diffraction, differential scanning calorimetry (DSC) and positron annihilation.

**EXPERIMENTS:**  $Zr_xCu_{90-x}Al_{10}$  ( $x=50, 55, 60, 65$ ) bulk amorphous alloys with 8 mm in diameter and 60 mm in length were prepared by a tilt casting technique. For positron annihilation measurements, alloy samples were cut into the size of about 0.5 mm thickness disk. 8 MeV electron irradiations with total dose of  $2 \times 10^{18}$  e/cm<sup>2</sup> was performed for these alloys at 320 K by LINAC at Research Reactor Institute, Kyoto University. During irradiation, samples were cooled in water flow path. Irradiated samples were examined by X-ray diffraction, positron annihilation lifetime and coincidence Doppler broadening measurements at room temperature. The positron annihilation lifetime spectra consist of more than  $1.0 \times 10^6$  counts. The positron lifetime spectra were analyzed by using POSITRONFIT program.

**RESULTS:** The mean positron lifetime  $\tau$  of all as-quenched sample was about  $165 \pm 2$  psec. Before irradiation, no difference of positron lifetime for different amorphous alloy systems was observed. This shows that open volume existing in amorphous is apparently same. However, the CDB spectra of these alloys before irradiation are not necessarily same. Take into account for these facts, it can be deduced that total electron density of open volume in any amorphous alloy is almost same but the real size of open space and chemical ratio around it depending on alloy composition is not same for various compositional alloys. Figure 1 shows the change in positron annihilation lifetime by electron irradiation as a function of Zr composition ratio in bulk amorphous alloys. It found that the increasing trend of positron lifetime becomes smaller with increasing of Zr contents. Especially, we found that radiation induced open volume change is suppressed in glassy alloys including more than 60% Zr atoms.

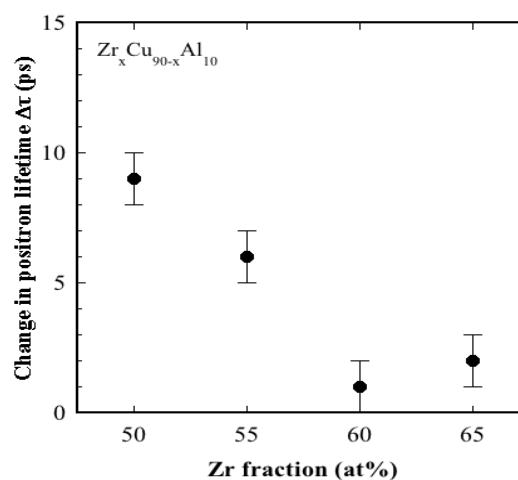


Fig. 1 Change of positron lifetime for various compositions of ZrCuAl bulk amorphous alloys by 8 MeV electron irradiation.

### REFERENCES

- [1] N.Onodera, A.Ishii, Y.Fukumoto, A.Iwase, Y.Yokoyama, and F.Hori, Nucl. Inst. & Meth. B. 282 (2012) 1
- [2] F.Hori, N.Onodera, A.Ishii, Y.Fukumoto, A.Iwase, A.Kawasuso, A.Yabuuchi, M.Maekawa and Y.Yokoyama, J. Phys.: Conf. 262 (2011) 012025



## PR6-8 Positron Annihilation Study of Fe-Cr Alloys after Neutron Irradiation in KUR

R. Kasada<sup>1</sup>, K. Sato<sup>2</sup>, Q. Xu<sup>3</sup>

<sup>1</sup>*Institute of Advanced Energy, Kyoto University*

<sup>2</sup>*Department of Mechanical Engineering, Kagoshima University*

<sup>3</sup>*Research Reactor Institute, Kyoto University*

**INTRODUCTION:** Ferritic steels containing Cr are expected to be used for the first-wall component of the fusion reactors as well as for the fuel pin cladding of the Generation IV nuclear fission systems [1]. However, high-Cr steels may suffer from thermal aging embrittlement, which is well-known 475 °C embrittlement. This is mainly due to hardening phenomenon through the phase separation of Fe and Cr as shown in the phase diagram. In the previous study [2], we applied a positron annihilation spectrometry to detect the phase separation in the Fe-Cr alloys after thermal aging at 475 °C.

The present collaborative research has investigate the neutron irradiation effect on the positron annihilation lifetime of Fe-Cr alloys.

**Experimental Procedure:** Materials used in the present study are Fe<sub>x</sub>Cr binary alloys. Neutron irradiation on these materials was carried out at 300 °C up to 199 h in KUR. The displacement damage is  $2.1 \times 10^{-3}$  dpa ( $5.1 \times$

$10^{18}$  n/cm<sup>2</sup>). Positron annihilation lifetime spectrometry was carried out for investigating open-volume type defects produced by irradiation.

**Results and Discussions:** Results of positron annihilation lifetime spectrometry is shown in Table 1. There is no meaningful difference in the mean lifetime of unirradiated Fe-Cr binary alloys. After the neutron irradiation in KUR, the mean lifetime of pure Fe and Fe-*x*Cr alloys for  $x \leq 85$  slightly increased but not decomposed into multi-components. On the other hand, that of Fe-91Cr and pure Cr showed two- and three components, respectively. This results indicate that Fe atom suppress vacancy cluster formation in the Fe-Cr binary alloys from a view of the Cr-rich side. Further investigation is needed for understanding the effect of Cr (or Fe) atom on the formation of vacancy type cluster in Fe-Cr alloys.

### REFERENCES:

- [1] A. Kimura, et al., Journal of Nuclear Science and Technology, 44 (2007) 323-328.  
 [2] R. Kasada and K. Sato, submitted to J. Alloys and Compounds.

Table 1 Results of positron annihilation lifetime spectrometry of Fe-Cr alloys before and after neutron irradiation in KUR.

Materials	Unirr.		Irr.				
	$\tau_m$ (ps)	$\tau_1$ (ps)	I1 (%)	$\tau_2$ (ps)	I2 (%)	$\tau_3$ (ps)	I3 (%)
Fe	104 ± 1	109 ± 1					
Fe-9Cr	107 ± 1	109 ± 1					
Fe-15Cr	105 ± 1	109 ± 1					
Fe-30Cr	105 ± 1	109 ± 1					
Fe-45Cr	105 ± 1	109 ± 1					
Fe-50Cr	105 ± 1	108 ± 1					
Fe-70Cr	105 ± 1	107 ± 1					
Fe-85Cr	104 ± 1	110 ± 1					
Fe-91Cr	105 ± 1	113 ± 1	93 ± 1	383 ± 9	7 ± 1		
Cr	103 ± 1	24 ± 4	9 ± 1	156 ± 2	48 ± 1	502 ± 3	43 ± 1

## PR6-9 Positron Annihilation Lifetime Measurements of Austenitic Stainless Steels Irradiated in the SINQ Target Irradiation Program

K. Sato, Q. Xu<sup>1</sup>, T. Yoshiie<sup>1</sup>, Y. Dai<sup>2</sup> and K. Kikuchi<sup>3</sup>

Graduate School of Science and Engineering, Kagoshima University

<sup>1</sup> Research Reactor Institute, Kyoto University

<sup>2</sup> Spallation Neutron Source Division, Paul Scherrer Institut

<sup>3</sup> Frontier Research Center for Applied Atomic Sciences, Ibaraki University

**INTRODUCTION:** Austenitic stainless steels have been known as highly corrosion resistant materials and important nuclear materials. There have been a number of studies on the void swelling behavior of them [1,2]. Recent theoretical and experimental analyses have revealed the importance of incubation period, a transient stage before the steady growth of voids. However, experimental results of void swelling in austenitic stainless steels have been limited to high dose. Because most of experimental studies have been performed by transmission electron microscopy after observable void formation, and point defects and their clusters under the resolution limits are impossible to detect. Therefore, point defect processes during the incubation period are not clear. In this study, the effect of alloying elements on defect structures in austenitic stainless steels and their model metals during the incubation period was studied after neutron irradiation by using positron annihilation lifetime measurement.

**EXPERIMENTS:** Titanium-doped 316-type austenitic stainless steel, called Japanese Primary Candidate Alloy (JPCA), and the reduced activated ferritic/martensitic steel F82H were used in this study. The JPCA was irradiated in the first SINQ (Swiss Spallation Neutron Source) target irradiation program (STIP-I). More details of the STIP-I experiments have been previously reported [3]. Irradiation position was F21. Irradiation temperature was 413K, and irradiation dose was 6.3dpa. After implementing a fatigue test on JPCA at room temperature, the positron annihilation lifetimes of the undeformed area of the sample were measured at the Research Reactor Institute, Kyoto University. A three-detector system using a fast digital oscilloscope and BaF<sub>2</sub> scintillators [4] was adopted for the positron annihilation lifetime measurements, thereby reducing the background counts and making it possible to measure highly radioactive samples. The time resolution of the system was 150 ps (full width at half maximum). Each spectrum was accumulated to a total of  $1.5 \times 10^6$  counts. The resulting spectra were analyzed using the PALSfit program [5]. The isochronal annealing of the positron annihilation lifetime was examined every

100 K from 423 to 1323 K. After annealing, samples were cooled down by air cooling. Cool time to room temperature was about 20 minutes.

**RESULTS:** Short and long lifetime component in the two component analysis was 150 (6) ps and 237 (7) ps, respectively. Intensity of short and long lifetime component was 49 (7) % and 51 (7) %, respectively. Errors are shown in parentheses. The long lifetimes result from the formation of vacancy-cluster-He-atom ( $V_m\text{-He}_n$ ) complexes (large open space defects), while the short lifetimes denote the formation of stacking fault tetrahedra (SFTs), dislocation loop, and single-vacancy-He-atom ( $V\text{-He}_n$ ) complexes (small open space defects). The experimental value of 230 ps is slightly smaller than the calculated positron lifetime of 249 ps for 4-vacancy clusters ( $V_4$ ) in Ni. Yet the vacancy cluster size is not likely to be less than 4, because many He atoms formed in the samples during irradiation. The positron lifetime of the He bubbles decreases as the number of He atoms in a vacancy cluster increases. Thus the exact vacancy cluster size cannot be determined, because they are too small to be directly observed by TEM.

The positron lifetime does not change after isochronal annealing up to 623 K. The spectra only show one component for annealing between 723 and 923 K, but they resolve into two components when annealed above 1023 K. It is expected that  $V_m\text{-He}_n$  complexes absorb He atoms by annealing at temperatures up to 623 K. Because the complexes incorporate many He atoms after irradiation, the lifetime decrease caused by absorption of helium may become saturated. In this stage, the He bubble concentration does not change because the long lifetime intensity is almost constant. SFTs and  $V\text{-He}_n$  complexes are expected to dissociate after annealing at 623 K. These defects, which have a short lifetime for annealing at up to 523 K, tend to aggregate and  $V_m\text{-He}_n$  complexes are formed. It is impossible to resolve them into two components. A small increase in the mean lifetime arises because of both the growth of  $V_m\text{-He}_n$  complexes and their release of H atoms. The  $V_m\text{-He}_n$  complexes dissociate after annealing at 1023 K. In this stage, the absorption of vacancies is larger than that of He atoms, and therefore, the long lifetime increases.

### REFERENCES:

- [1] F.A. Garner, Materials Science and Technology, Vol. 10 (VCH Weinheim, 1994), p. 419.
- [2] T. Okita *et al.*, J. Nucl. Mater. **307-311** (2002) 322.
- [3] Y. Dai and G.S. Bauer, J. Nucl. Mater. **296** (2001) 43.
- [4] H. Saito *et al.*, Nucl. Instr. Meth. Phys. Res. A **487** (2002) 612.
- [5] J.V. Olsen *et al.*, Phys. Stat. Sol. C **4** (2007) 4004.

採択課題番号 26P6-12 電子照射と中性子照射によって形成した金属中の格子欠陥と プロジェクト  
ガス原子の相互作用の解明

(鹿児島大院・理工) 佐藤紘一 (京大・原子炉) 徐虬、義家敏正 (九大・応力研) 大澤一人  
(産総研) 大島永康

# PR6-10 Effects of High Energy Particle Irradiation on Hydrogen Retention in Refractory Metals

K. Tokunaga, M. Matsuyama<sup>1</sup>, S. Abe<sup>1</sup>, H. Osaki<sup>2</sup>, K. Araki, T. Fujiwara, M. Hasegawa, K. Nakamura, Q. Xu<sup>3</sup> and K. Sato<sup>3</sup>

Research Institute for Applied Mechanics, Kyushu University

<sup>1</sup>Hydrogen Isotope Research Center, University of Toyama

<sup>2</sup>Interdisciplinary Graduate School of Engineering Sciences, Kyushu University

<sup>3</sup>Research Reactor Institute, Kyoto University

**INTRODUCTION:** It is of importance to clarify phenomena of implantation, retention, diffusion and permeation of tritium on surface of the armor materials of the first wall/blanket and the divertor on fusion device from a viewpoint of precise control of fuel particles, reduction of tritium inventory and safe waste management of materials contaminated with tritium (T). Refractory metals such as tungsten (W) is potential candidate for an armor of the first wall and the divertor plate of the fusion reactor because of its low erosion yield and good thermal properties. The armor material will be subjected to heavy thermal loads in the steady state or transient mode combined with high energy neutron irradiation that will cause serious material degradation. In addition, high energy runaway electrons would bombard the armor materials along the equatorial plane in fusion device. It is considered that these cause radiation damage and enhance tritium retention. In the present works, T exposure experiments have been carried out on W samples which were irradiated by high energy electrons using LINAC in KURRI of Research Reactor Institute, Kyoto University to investigate effects of high energy electrons irradiation and microstructure on tritium retention of W.

**EXPERIMENTS:** W samples used in the present experiments were two oriented ITER grade W. One was W sample (ITER grade W(1)) which the surface were manufactured to be oriented parallel to the rolling surface and rolling direction. The other was W sample (ITER grade W(3)) which the surface were manufactured to be oriented perpendicular to the rolling surface and rolling direction. The sizes of W samples were 10mm x 10mm x 1mm. The surface of the both samples were polished to be mirrored. High energy electrons irradiation has been carried out using LINAC in KURRI of Research Reactor Institute, Kyoto University. An energy of electron irradiated was 10 MeV and DPA was  $3.26 \times 10^{-3}$ . Temperature during the irradiation was measured by thermocouples which was contacted with a backside of the W samples. After the electron beam irradiation, T exposure experiments have been carried out using a T exposure device in University of Toyama. Pressure of the T gas was 1.3 kPa and T exposure was kept for 4 h. T concentration in the

gas was about 5 %. Temperatures of pre-heating and T exposures were 100 °C. After the exposure to T gas, T amount retained in surface layers of the sample was evaluated by  $\beta$ -ray-induced X-ray spectrometry (BIXS) and imaging plate (IP) measurements.

**RESULTS:** Temperature of the W samples during the electron irradiation was 85 °C. Figure 1 shows the result of the IP measurement of ITER grade W(1) (IG W(1)) and ITER grade W(3)(IG W(3)). The IP images indicate that amount of T on the surface of IG W(3) is larger than that of the surface of IG W(1). Comparison with the standard samples shows that amount of T of the surface of IG W(1) and IG W(2) are 0.0604 kBq/mm<sup>2</sup> and 0.166 kBq/mm<sup>2</sup>, respectively. Figure 2 show line analyses of PLS value of the surface of IG W(3) (a) and IG W(1) (b) after the T exposure. It can be seen that line profiles are almost constant. These result indicates that T is easy to diffuse parallel direction for rolling direction. Electron beam irradiation effect will be discussed by comparing with the result of un-irradiated W samples.

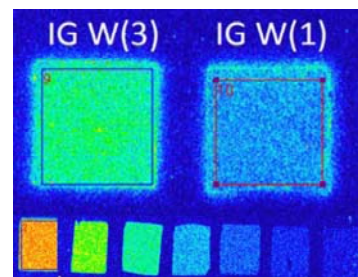


Fig. 1. Tritium image of ITER grade W(3) (IG W(3)) and ITER grade W(1)(IG W(1)). Bottom parts are standard samples.

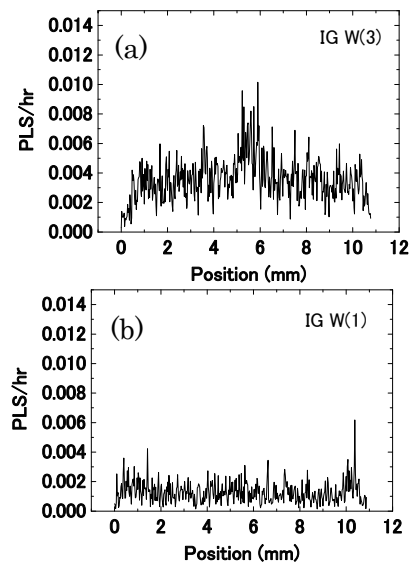


Fig. 2. Line analyses of IG W(3) (a) and IG W(1) (b) after tritium exposure.

採択課題番号 26P6-13

高融点金属における水素吸蔵特性に及ぼす  
高エネルギー粒子線照射効果

プロジェクト

(九大・応用研) 徳永和俊、荒木邦明 (九大・総理工) 尾崎浩詔 (京大・原子炉) 徐 虬、佐藤紘一

N. Nitta<sup>1</sup>, C. Watanabe<sup>1</sup>, M. Taniwaki<sup>1</sup>, Q. Xu<sup>2</sup>, T. Yoshiie<sup>2</sup>

<sup>1</sup>*School of Environmental Science and Engineering,  
Kochi University of Technology*

<sup>2</sup>*Research Reactor Institute, Kyoto University*

**INTRODUCTION:** Fine cellular structure is formed on GaSb, InSb and Ge semiconductors by ion irradiation as shown by Fig. 1[1]-[6]. The authors proposed an idea that this structure is formed by the behavior of point defects induced by ion irradiation, that is, first the voids form from the oversaturated vacancies and they develop by absorbing point defects induced continuously during ion irradiation. This idea has been proved by intense studies on the ion dose dependence and temperature dependence of the cellular structure. However, the authors do not have detailed understanding over all the cell formation process. Especially, the details of the formation mechanism of voids are not yet clear. Though the authors have surely observed the voids prior to the development of the cellular structure, the diameter of these voids are so large (30-50 nm) and the smaller voids are not yet found, then large voids appear suddenly during ion irradiation, not developing from small voids. Therefore another effect on voids formation, for example, the thermal spike, is suspected. Thermal spike effect depends on the mass of ions, then, the authors aim to investigate the ion mass dependence of the voids formation and development in this work. In addition, the chemical effect of implanted ions is studied.

**EXPERIMENTS:** The GaSb (001) wafers were implanted by C, Si, Ge, Pb (IV elements as Sn), Al and P ions by accelerated by 60 kV voltage to the dose of  $10^{15}$  ions/cm<sup>2</sup>. The wafers were kept at 100-110 K during ion irradiation. The surface morphology of the implanted wafers was observed by a FE-SEM.

**RESULTS:** Voids removed their top surfaces were observed on the relatively large mass ions (Ge and Pb) irradiated wafer surfaces, and they were scarcely formed the small mass ions (Si and Al) irradiated surfaces.

In the case of Pb with the largest atom mass (207.2), the diameter of voids was widely distributed from 10 nm - 300 nm. The density of voids with a diameter of 100 nm and over are  $4.4/1 \mu\text{m}^2$ , and they are formed by coalesce of neighboring voids (these void diameters are less than about 100 nm), consequently, the maximum diameter of individual voids is 100 nm at most.

Most of the voids observed in Ge (atomic mass =72.64)

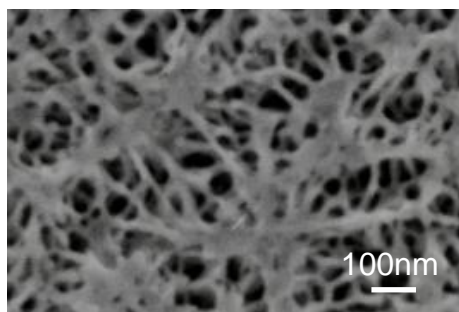


Fig. 1. FE-SEM image of GaSb surface by 60 keV Sn<sup>+</sup> implanted GaSb to a dose of  $1.2 \times 10^{15}$  ions/cm<sup>2</sup> at 150 K.

irradiated sample have small diameters less than 30 nm, but some of the voids (the density is about  $2/1 \mu\text{m}^2$ ) have about 100 nm diameter. These relatively large voids are removed their top surfaces but seem to consist of single void.

In Si irradiated wafer, some small contrasts which might show the voids were observed, and their density was about  $2/1 \mu\text{m}^2$ . However, in Al ion irradiated samples, the void contrast was not observed. These atom masses are so small (26.98 and 28.09) that the ion range is large and distribution is wide, therefore it is considered that the point defects density is too small for voids formation and development.

By SEM study which has been performed until now, it was assured that the atomic mass of irradiated ion affects the voids formation and development. However, from SEM study we cannot know much under the surface, then, the details are not yet clarified. The authors will study under the surface by cross-sectional TEM in order to understand the void formation mechanism.

#### REFERENCES:

- [1] 新田紀子, 谷脇雅文, 鈴木朝夫, 林 禎彦, 佐藤裕樹, 義家敏正, 日本金属学会誌, **64** (2000), 1141-1147.
- [2] N. Nitta, M. Taniwaki, T. Suzuki, Y. Hayashi, Y. Satoh and T. Yoshiie, Materials Transactions, **43** (2002), 674-680.
- [3] N. Nitta, M. Taniwaki, Y. Hayashi and T. Yoshiie, J. Appl. Phys., **92** (2002), 1799-1802.
- [4] N. Nitta, M. Taniwaki, Y. Hayashi and T. Yoshiie, Physica B, **376-377** (2006), 881-885.
- [6] N. Nitta, T. Hasegawa, H. Yasuda, Y. Hayashi, T. Yoshiie, and M. Taniwaki, Materials Transactions **52**, (2011) 127-129.